

SHORT REPORT

Distinct mechanisms controlling rough and smooth endoplasmic reticulum contacts with mitochondria

Peter T. C. Wang^{1,*}, Pierre O. Garcin^{2,*}, Min Fu^{1,*}, Matthew Masoudi¹, Pascal St-Pierre¹, Nelly Panté² and Ivan R. Nabi^{1,‡}

ABSTRACT

Gp78 (also known as AMFR), an endoplasmic-reticulum (ER)-associated protein degradation (ERAD) E3 ubiquitin ligase, localizes to mitochondria-associated ER and targets the mitofusin (Mfn1 and Mfn2) mitochondrial fusion proteins for degradation. Gp78 is also the cell surface receptor for autocrine motility factor (AMF), which prevents Gp78-dependent mitofusin degradation. Gp78 ubiquitin ligase activity promotes ER–mitochondria association and ER–mitochondria Ca^{2+} coupling, processes that are reversed by AMF. Electron microscopy of HT-1080 fibrosarcoma cancer cells identified both smooth ER (SER; ~8 nm) and wider (~50–60 nm) rough ER (RER)–mitochondria contacts. Both short hairpin RNA (shRNA)-mediated knockdown of Gp78 (shGp78) and AMF treatment selectively reduced the extent of RER–mitochondria contacts without impacting on SER–mitochondria contacts. Concomitant small interfering RNA (siRNA)-mediated knockdown of Mfn1 increased SER–mitochondria contacts in both control and shGp78 cells, whereas knockdown of Mfn2 increased RER–mitochondria contacts selectively in shGp78 HT-1080 cells. The mitofusins therefore inhibit ER–mitochondria interaction. Regulation of close SER–mitochondria contacts by Mfn1 and of RER–mitochondria contacts by AMF-sensitive Gp78-mediated degradation of Mfn2 define new mechanisms that regulate ER–mitochondria interactions.

KEY WORDS: AMF, Gp78 E3 ubiquitin ligase, ER-mitochondria contacts, Ca^{2+} coupling, Mitofusin

INTRODUCTION

Close contacts between the ER and mitochondria regulate multiple cellular processes including Ca^{2+} signaling and homeostasis, phospholipid and sterol biosynthesis, and mitochondrial biogenesis and metabolism, as well as the execution of cell death programs (Lynes and Simmen, 2011; Rowland and Voeltz, 2012). ER–mitochondria tethers include the Mmm1–Mdm10–Mdm12–Mdm34 tethering complex, phosphofurin acidic cluster sorting protein 2 (PACS-2), inositol triphosphate receptor (IP₃R), voltage-dependent anion-selective channel (VDAC) Ca^{2+} channels and the mitochondrial fusion protein Mfn2 (de Brito and Scorrano, 2008; Kornmann et al., 2009; Rapizzi et al., 2002; Simmen et al., 2005; Szabadkai et al., 2006). In yeast, a SKP1–cullin-1–F-box (SCF) ubiquitin ligase complex regulates ER–mitochondria phospholipid

transport (Schumacher et al., 2002). However, a ubiquitin ligase function in the ER–mitochondria interaction in mammalian cells has yet to be reported. Here, we describe a new mechanism linking extracellular regulation of the ER-localized Gp78 E3 ubiquitin ligase (also known as AMFR) to ER–mitochondria interaction.

Gp78, an ER membrane-anchored ubiquitin ligase (E3), is a central component of the endoplasmic-reticulum (ER)-associated protein degradation (ERAD) machinery (Christianson et al., 2011; Fang et al., 2001; Song et al., 2005; Ye et al., 2005; Zhong et al., 2004). Gp78 is also the cell surface receptor for autocrine motility factor (AMF), the same protein as the glycolytic enzyme phosphoglucose isomerase (PGI), which functions upon non-classical secretion as a cytokine, promoting cancer cell motility and metastasis through Gp78 (Nabi et al., 1990; Silletti et al., 1991). As assessed by electron microscopy, the Gp78-specific 3F3A monoclonal antibody (mAb) localizes Gp78 to both the plasma membrane and smooth ER (SER) tubules whose association with mitochondria is regulated by free cytosolic Ca^{2+} ($[Ca^{2+}]_{cyt}$) (Benlimame et al., 1998, 1995; Goetz et al., 2007; Wang et al., 2000). The ER is associated with mitochondrial fission sites (Friedman et al., 2011) and Gp78 ubiquitin ligase activity targets the mitochondrial fusion proteins, mitofusin 1 (Mfn1) and Mfn2, for degradation inducing mitochondrial fission and, upon mitochondrial depolarization, mitophagy (Fu et al., 2013). Dynamin- and Rac1–PI3K-dependent raft internalization of AMF to the Gp78-positive ER prevents Gp78 degradation of the mitofusins and reverses Gp78-dependent mitochondrial fission (Kojic et al., 2007; Le et al., 2002; Shankar et al., 2013).

Analysis of ER–mitochondria overlap and Ca^{2+} coupling in Mfn1- and Mfn2-knockout mouse embryonic fibroblasts (MEFs) has suggested that ER-associated Mfn2 interacts with mitochondrial Mfn1 and Mfn2 to form an ER–mitochondria tether (de Brito and Scorrano, 2008). However, electron microscopy analysis has shown that ER–mitochondria contact increases in Mfn2-knockout MEFs (Cosson et al., 2012). and, more recently, also enhances ER–mitochondria Ca^{2+} crosstalk, sensitizing the cells to mitochondrial Ca^{2+} cell death (Filadi et al., 2015). Here, we study the role of AMF and Gp78, and their mediation of mitofusin degradation, in the regulation of ER–mitochondria interaction.

RESULTS AND DISCUSSION

AMF–Gp78 regulation of ER–mitochondria association

To test whether Gp78 expression affected ER–mitochondria contacts, Cos7 cells were transfected with Flag–Gp78 or its Ring finger mutant Gp78 (Flag–Gp78-RFmut), which lacks ubiquitin ligase activity, and labeled for syntaxin-17, a mitochondria-associated ER marker (Hamasaki et al., 2013), and for the mitochondrial OxPhosV complex. 3D spinning disk confocal stacks show close opposition of the syntaxin-17-labeled ER and mitochondria (Fig. 1A). Quantification of syntaxin-17–

¹Departments of Cellular and Physiological Sciences, Life Sciences Institute, University of British Columbia, Vancouver, British Columbia, Canada V6T 1Z3.

²Department of Zoology, Life Sciences Institute, University of British Columbia, Vancouver, British Columbia, Canada V6T 1Z3.

*These authors contributed equally to this work

‡Author for correspondence (irnabi@mail.ubc.ca)

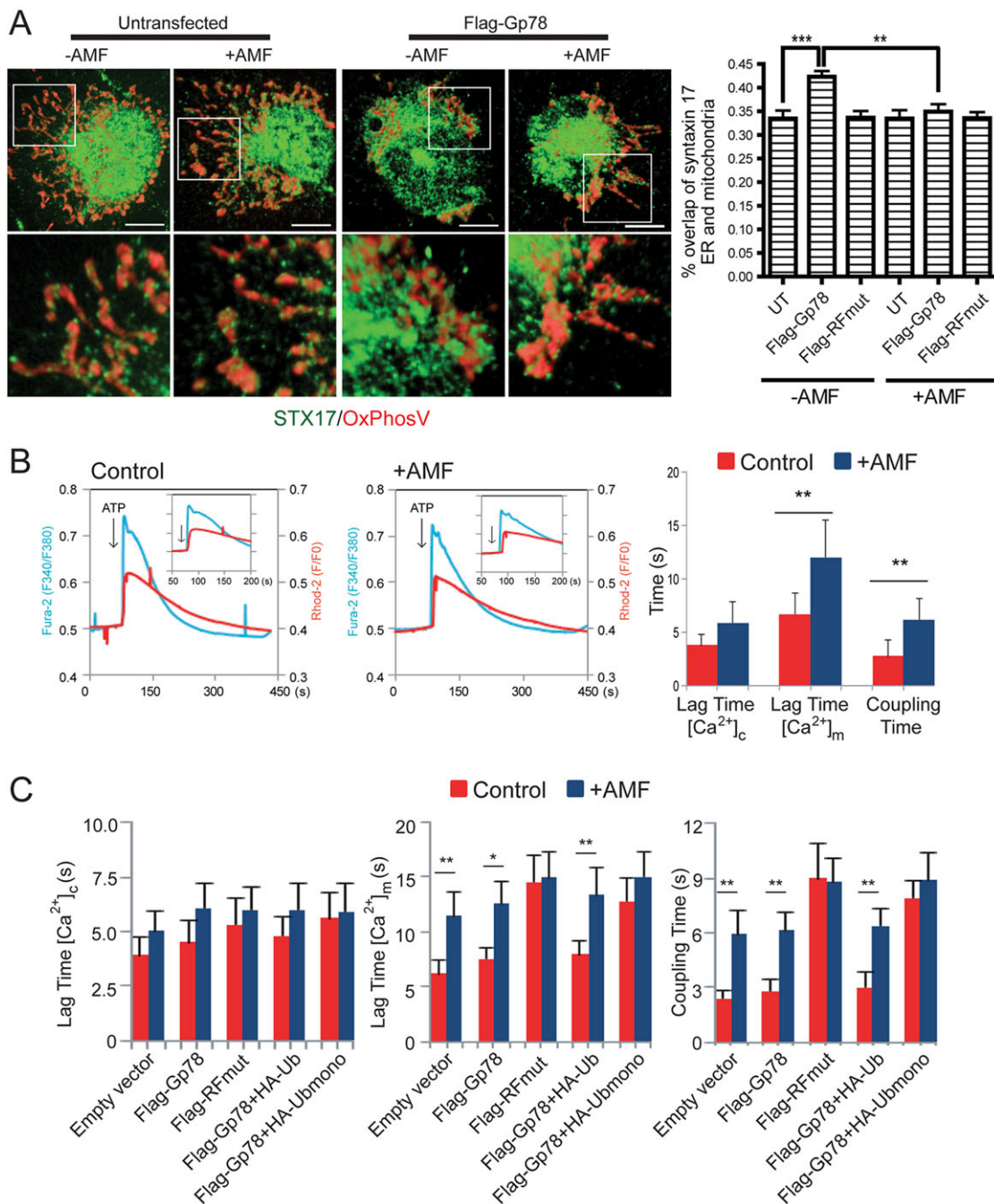


Fig. 1. AMF-Gp78 control of ER-mitochondria association and Ca²⁺ coupling. (A) 3D reconstructed images of Flag-Gp78- or Flag-RINGmut-transfected Cos7 cells labeled for OxPhosV (red) and syntaxin-17 (green). Cells were either untreated or treated with AMF (+AMF; 2 h) and overlap of syntaxin-17 and mitochondrial volume was quantified. Results are mean±s.e.m. (*n*=25–30). ***P*<0.01. Scale bars: 10 μm. (B) Simultaneous recording of Cos7 cells loaded with ATP-evoked [Ca²⁺]_{cyt} and [Ca²⁺]_m in Fura-2-AM (light blue) and Rhod-2-AM (red) with (right) or without (left) AMF treatment. The bar graph shows the lag time of ATP-induced [Ca²⁺]_{cyt} and [Ca²⁺]_m and ER-mitochondria Ca²⁺ coupling times. Results are mean±s.e.m. (*n*=60–90). **P*<0.05, ***P*<0.01. (C) Cos7 cells were transfected with Flag-4c-Gp78 or Flag-4c-RINGmut or co-transfected with Flag-4c-Gp78 with HA-Ub or HA-Ubmono. Bar graphs show the lag time of ATP-induced [Ca²⁺]_{cyt} (left) and [Ca²⁺]_m (middle) and ER-mitochondria Ca²⁺ coupling times (right) with (blue) or without (red) AMF treatment. Results are mean ±s.e.m. (*n*=20–30). **P*<0.05, ***P*<0.01.

mitochondria overlap showed that Gp78 significantly increased ER-mitochondria contacts, an effect that was prevented by Gp78 Ring finger mutation and reversed by treatment with AMF.

To study ER-mitochondrial Ca²⁺ coupling, Cos7 cells were loaded with both Fura-2-AM and Rhod-2-AM and the ATP-induced increase of [Ca²⁺]_{cyt} and [Ca²⁺]_m measured simultaneously (Pacher et al., 2008). ATP stimulation induced a steep rise in [Ca²⁺]_{cyt}

closely followed by a synchronous rise in [Ca²⁺]_m indicative of the rapid and efficient delivery of Ca²⁺ from ER to mitochondria. AMF pretreatment delayed ATP-induced [Ca²⁺]_m but not [Ca²⁺]_{cyt} signals (Fig. 1B).

Cos7 cells transfected with tetracysteine motif (4c)-tagged Gp78-wild type or RFmut were identified using FIAsh, which fluoresces upon binding to the tetracysteine motif (Adams et al., 2002). Using

Ca²⁺ imaging of Fura-2 and Rhod-2 double-labeled cells, AMF delays propagation of the ATP-evoked [Ca²⁺]_{cyt} rise to mitochondria in both empty vector and Flag-Gp78 wild-type transfected cells (Fig. 1C). Flag-RFmut expression significantly prolongs ER-mitochondria coupling times that are no longer impacted by AMF (Fig. 1C). Similarly, co-transfection of Flag-Gp78wt with mutated HA-tagged ubiquitin (K29R, K48R and K63R, denoted HA-Ubmono), preventing Gp78-dependent polyubiquitin chain elongation (St-Pierre et al., 2012), results in longer and AMF-insensitive coupling times (Fig. 1C). Gp78 ubiquitin ligase activity therefore promotes AMF-sensitive ER-mitochondria contacts and Ca²⁺ coupling.

AMF-Gp78 selectively regulate RER-mitochondria contacts

To study Gp78-mediated regulation of ER-mitochondria interaction by electron microscopy, we stably transfected HT-1080 fibrosarcoma cells, which express elevated levels of endogenous Gp78 (St-Pierre et al., 2012; Tsai et al., 2007), with doxycyclin-inducible Gp78 short hairpin RNA (shRNA; shGp78). 3D confocal analysis showed that shGp78 knockdown reduced syntaxin-17 overlap with mitochondria (Fig. 2A). Electron microscopy analysis

showed that the mitochondrial area increased upon Gp78 knockdown (Fig. 2B), consistent with the increased Mfn1 and Mfn2 levels and mitochondrial fusion observed in these cells (Shankar et al., 2013). Quantification of the mitochondria-associated ER identified closely opposed (8.0±0.5 nm, mean±s.e.m.) SER interactions and wider (50.5±1.7 nm) interactions with rough ER (RER) tubules presenting ribosomes facing the mitochondria surface (Fig. 2B). Similarly, ~10 nm SER- and ~25 nm RER-mitochondria contacts have been reported by studies using electron microscopy tomography to analyze rat liver (Csordas et al., 2006). In HT-1080 fibrosarcoma cells, RER contacts covered approximately twice the mitochondrial surface area as the SER contacts. shRNA Gp78 knockdown did not affect SER contacts but reduced by approximately half the mitochondrial surface area covered by RER contacts (Fig. 2B).

As for Gp78-transfected Cos7 cells, AMF reduced syntaxin-17-mitochondria contacts in HT-1080 cells (Fig. 3A). As assessed using electron microscopy, Gp78 knockdown did not increase the mitochondrial area in serum-starved HT-1080 cells; however, AMF treatment significantly increased mitochondrial area in control shRNA (shCtl) cells and not shGp78 knockdown cells (Fig. 3B).

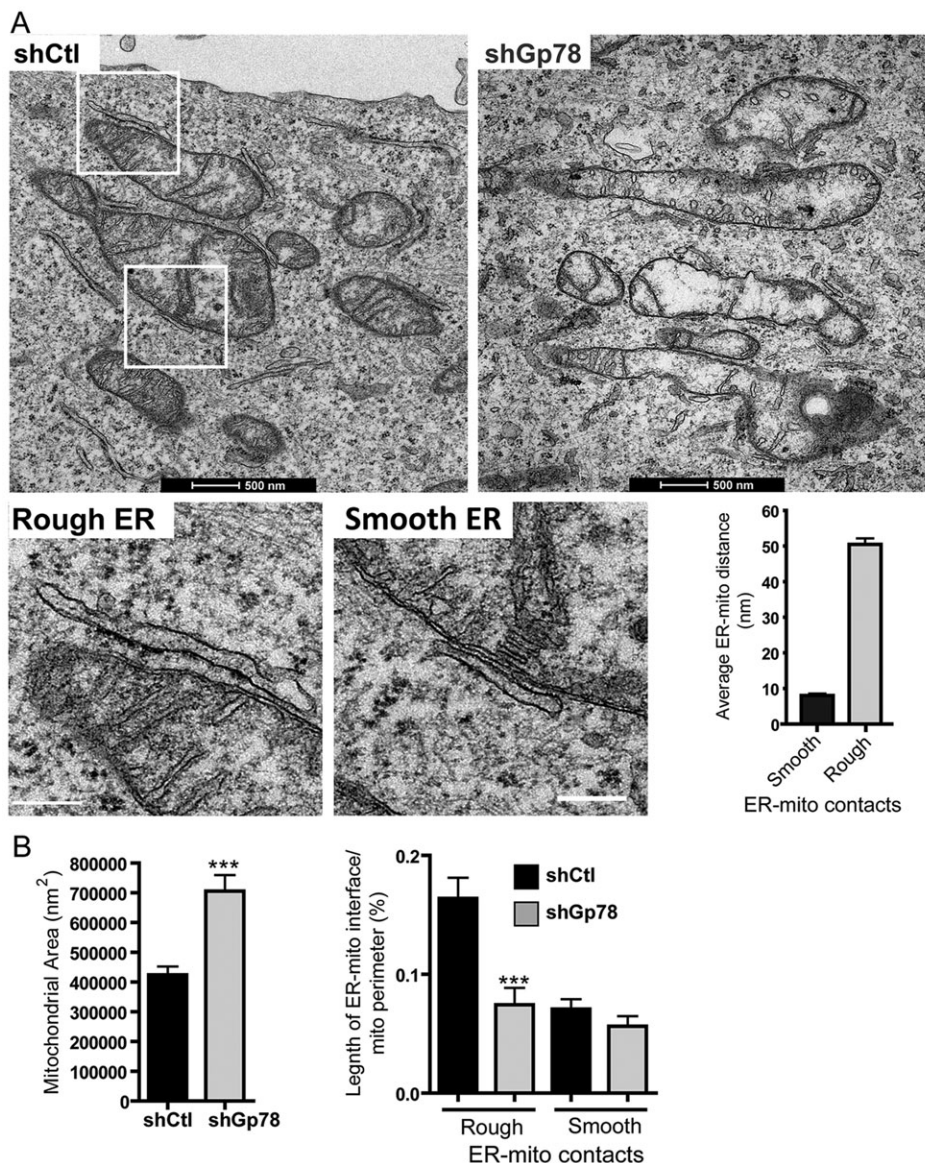


Fig. 2. Gp78 promotes the formation of RER-mitochondria contacts.

(A) Electron microscopy of shCtl and shGp78 HT-1080 cells. Insets show close contacts between RER (top) and SER (bottom) and mitochondria. The bar graph shows the width of rough and smooth contacts (mean±s.e.m.; *n*=50). Scale bars: 500 nm; insets, 200 nm. (B) Bar graphs show average mitochondrial area for shCtl and shGp78 HT-1080 cells (mean±s.e.m.) and the percentage of mitochondrial membrane interfacing with RER or SER contact sites (mean±s.e.m.; *n*≥167). ****P*<0.001.

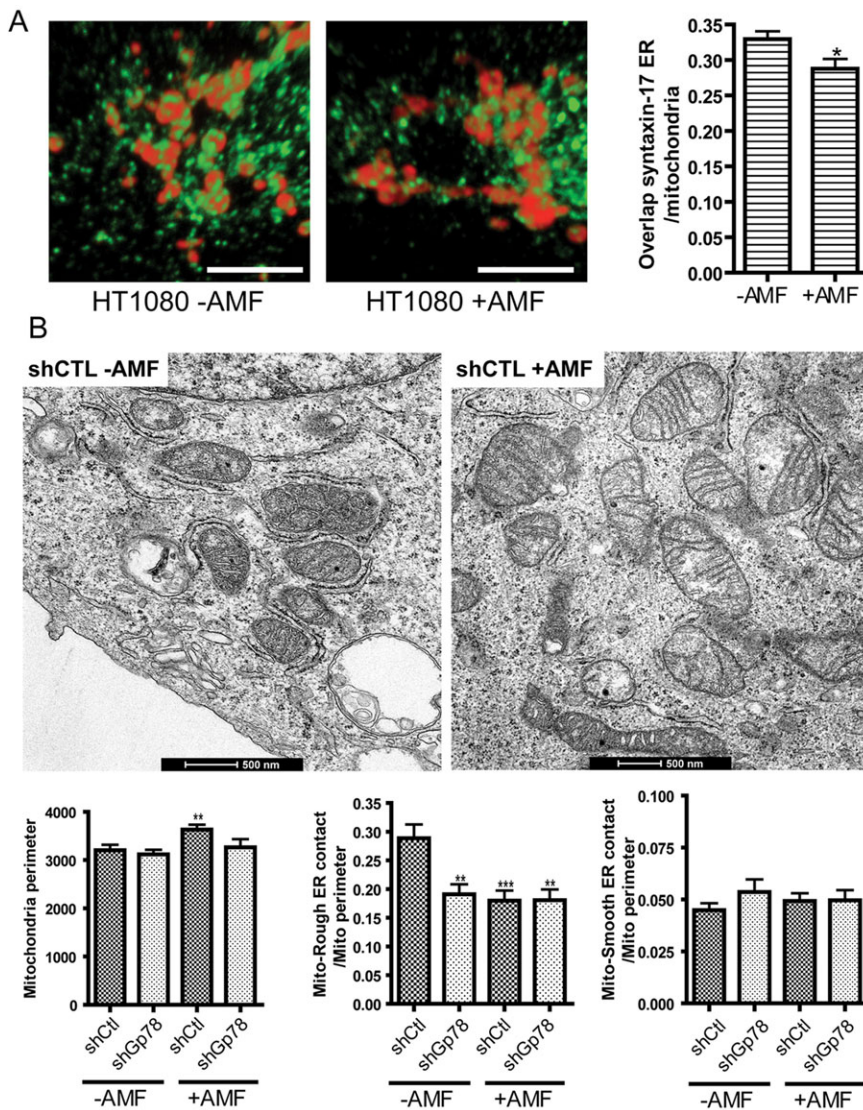


Fig. 3. AMF selectively disrupts RER–mitochondria contacts. (A) 3D reconstructed immunofluorescence images of HT-1080 cells untreated or treated with AMF and labeled for syntaxin-17 (green) and OxphosV (red). Scale bar: 10 μ m. The bar graph shows the percentage of mitochondrial volume overlapped by syntaxin-17. Results are mean \pm s.e.m. ($n=25$ –30). * $P<0.05$. (B) Representative electron microscopy images of serum-starved shCtl HT-1080 cells untreated and treated with AMF for 2 h. Scale bar: 500 nm. Bar graphs show average mitochondrial perimeter and the percentage of mitochondrial surface interfacing with either RER or SER contact sites (mean \pm s.e.m., $n \geq 162$). ** $P<0.01$; *** $P<0.001$.

Paralleling the reduction of ~ 50 nm RER contacts in shGp78 knockdown cells, AMF treatment reduced RER contacts in shCtl cells and did not affect the extent of SER contacts. AMF did not affect RER contacts in shGp78 knockdown cells and neither Gp78 knockdown nor AMF treatment impacted SER contacts (Fig. 3B). AMF reversal of Gp78-dependent mitofusin degradation and mitochondrial fission (Shankar et al., 2013) is therefore mediated by AMF disruption of Gp78-dependent ER–mitochondria contacts, defining a new mechanism whereby an extracellular cytokine regulates mitochondrial dynamics through control of ER–mitochondria interaction.

Role of mitofusins

Gp78 targets both Mfn1 and Mfn2 for proteasomal degradation (Fu et al., 2013). Reduced RER–mitochondria contacts in shGp78 HT-1080 cells is therefore associated with elevated levels of both Mfn1 and Mfn2. Mfn1 or Mfn2 small interfering RNA (siRNA)-mediated knockdown reduced mitofusin levels in both shCtl and shGp78 cells. Mfn1 or Mfn2 knockdown did not affect the extent of syntaxin-17 ER–mitochondria contacts in shCtl cells but, surprisingly, both knockdowns induced a significant increase in contacts in shGp78 HT-1080 cells (Fig. 4A). Electron microscopy analysis showed that Mfn1 or Mfn2 knockdown reduced

mitochondrial size. Mfn1 knockdown did not significantly affect RER–mitochondria contacts in shCtl or shGp78 HT-1080 cells, but more than doubled SER–mitochondria contacts in both cell lines. Mfn2 knockdown impacted on neither rough nor smooth contacts in shCtl cells, but increased RER contacts in shGp78 HT-1080 cells (Fig. 4B). This suggests that, in the HT-1080 cells studied here, Mfn1 and Mfn2 mediate distinct mechanisms that inhibit formation of SER– and RER–mitochondria contacts, respectively.

New mechanisms of ER–mitochondria interaction

Regulation of RER–mitochondria association through AMF-mediated regulation of the Gp78 ubiquitin ligase defines a new mechanism to regulate association between these two organelles. The ~ 8 -nm SER contacts and ~ 50 -nm RER contacts that we observed in HT-1080 fibrosarcoma cells were similar to those previously reported in rat liver (Csordas et al., 2006). In the HT-1080 fibrosarcoma cells studied here, Mfn1 and Mfn2 selectively inhibited formation of SER– and RER–mitochondria contacts, respectively. How this relates to the distinct roles of Mfn1 and Mfn2 in mitochondrial fusion and the recently described role of Mfn2 in mitochondrial metabolism remains to be determined (Ishihara et al., 2004; Mourier et al., 2015).

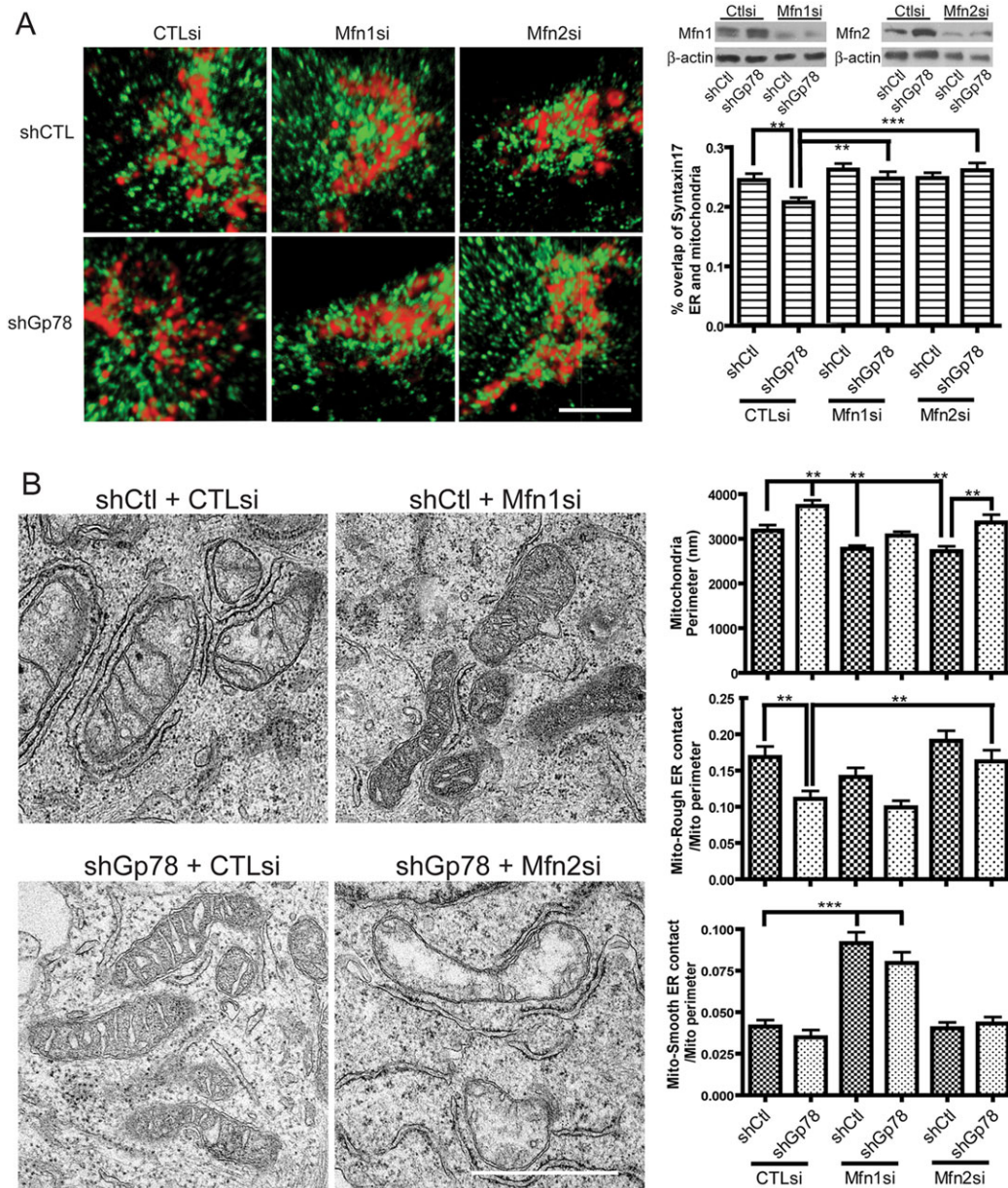


Fig. 4. Mitofusins 1 and 2 mediate distinct mitochondrial ER contacts. (A) 3D reconstructed confocal stacks of shCTL and shGp78 cells labeled for syntaxin-17 (green) and OxphosV (red) transfected with control (CTLsi), Mfn1 (Mfn1si) or Mfn2 (Mfn2si) siRNA. Scale bar: 10 μ m. Western blot of Mfn1, Mfn2 and β -actin in shCTL and shGp78 cells transfected with Mfn1 and Mfn2 siRNA. The bar graph shows the percentage of mitochondrial volume overlapped by syntaxin-17. Results are mean \pm s.e.m. ($n=25-30$). ** $P<0.01$, *** $P<0.001$. (B) Electron microscopy of shCTL cells transfected with control or Mfn1 siRNA and shGp78 cells transfected with control or Mfn2 siRNA. Scale bar: 1 μ m. Bar graphs show average mitochondrial perimeter and the percentage of mitochondrial membrane interfacing with RER or SER contact sites for shCTL and shGp78 HT-1080 cells transfected with control, Mfn1 or Mfn2 siRNA. Results are mean \pm s.e.m. ($n\geq 150$). ** $P<0.01$, *** $P<0.001$.

In contrast to its reported role as an ER–mitochondria tether (de Brito and Scorrano, 2008), we observed that Mfn2 siRNA increased ER–mitochondria contacts and, specifically, RER contacts in shGp78 cells. This suggests that Mfn2 inhibits ER–mitochondria contacts, supporting the conclusions reached in analysis of Mfn2^{-/-}MEFs (Cosson et al., 2012; Filadi et al., 2015). Gp78 might promote ER–mitochondria interaction through degradation of Mfn2 and removal of an inhibitor of contact formation. Intriguingly, Mfn1 knockdown increased SER–mitochondria contacts, even in control HT-1080 cells that express reduced Mfn1 levels. Mfn1 knockdown also prevents Gp78-dependent mitophagy, associated with recruitment of the autophagy protein LC3 to the mitochondria-

associated ER, the source of the autophagosome isolation membrane (Fu et al., 2013; Hamasaki et al., 2013). Mitochondrial fusion protects mitochondria from autophagy (Rambold et al., 2011); however, the selective protection accorded by Mfn1 knockdown, associated with mitochondrial fission, argues that control of ER–mitochondria contact sites might also influence the mitophagic process.

AMF has established pro-survival functions (Fu et al., 2011; Tsutsumi et al., 2003) and its regulation of Ca²⁺ homeostasis and mitochondrial fission through ER–mitochondria coupling has important implications for the role of this ubiquitous cytokine in various cellular processes, including tumor cell survival. Rough mitochondria-associated ER tubules present ribosomes facing

mitochondria and might be associated with translocon-mediated ER-mitochondria Ca^{2+} coupling (Flourakis et al., 2006). Indeed, as a key component of ERAD, Gp78 interacts with many components of the translocon, including derlin-1, VIMP and PNGase (Ballar et al., 2007; Li et al., 2006; Ye et al., 2005). Selective regulation of RER contact sites by AMF and Gp78 represents, to our knowledge, the first identified regulator of these contact sites.

Syntaxin-17 is a SNARE protein that is enriched at mitochondria-associated ER (Hamasaki et al., 2013) and represents a useful ER marker for light microscopy assessment of ER-mitochondria interaction. Nevertheless, confocal analysis of the proximity of syntaxin-17 to mitochondria was unable to distinguish alteration in SER and RER contacts associated with Mfn1 and Mfn2 knockdown, respectively. Similarly, whereas AMF treatment increased Ca^{2+} coupling times in untransfected Cos7 cells, we could not detect significant effects of AMF on syntaxin-17 ER-mitochondria interaction. Furthermore, expression of Gp78 enhanced syntaxin-17 ER-mitochondria contacts but did not significantly affect Ca^{2+} coupling, whereas expression of the Gp78 Ring finger mutant disrupted Ca^{2+} coupling without significantly affecting syntaxin-17 ER-mitochondria contacts. These data highlight the discordance between different approaches to measure ER-mitochondria contacts, the importance of ultrastructural analysis and also the diverse mechanisms that impact on contact formation and functional interaction between these two organelles. The contribution of both RER- and SER-mitochondria contact sites to the role of ER-mitochondria interaction in Ca^{2+} homeostasis, autophagy and apoptosis should be considered.

MATERIALS AND METHODS

Antibodies and chemicals

Rat IgM 3F3A anti-Gp78 mAb was as described previously (Nabi et al., 1990). Anti-OxPhosV antibodies were from Molecular Probes or Abcam, M2 anti-Flag and syntaxin-17 antibodies from Sigma, Mfn1 and Mfn2 antibodies from Santa Cruz Biotechnology, cross-adsorbed anti-rat IgM secondary antibody from Jackson ImmunoResearch Laboratories, and anti-mouse-IgG and anti-rabbit-IgG secondaries from Molecular Probes. Rhod-2-AM and pluronic F-127 (PAC) were from Invitrogen. PGI, ATP, Fura-2-AM and others were from Sigma.

Cell culture, constructs and treatments

Cos7 cells were grown in complete Dulbecco's modified Eagle's medium (DMEM) and transfected using Effectene (Qiagen). Stable HT-1080 clones expressing control shCt1 and Gp78-targeted shGp78 shRNAs (corresponding to sh6 Gp78 shRNA in Shankar et al., 2013) in doxycyclin-inducible pTRIPZ plasmid were maintained in medium containing 2 mg/ml puromycin and 1 mg/ml doxycyclin to induce Gp78 knockdown. For AMF treatment, cells were serum starved overnight and incubated with fresh medium containing 24 $\mu\text{g}/\text{ml}$ AMF.

Immunofluorescence

Flag-Gp78-transfected Cos7 cells were fixed with pre-cooled methanol-acetone and labeled with rat 3F3A, mouse OxPhosV and rabbit syntaxin-17 antibodies and secondary antibodies conjugated to Alexa Fluor 488, 568 and 647. Peripheral ER 3F3A labeling identified Flag-Gp78-transfected cells (St-Pierre et al., 2012). HT-1080 cells (expressing RFP) were labeled with mouse OxPhosV mAb and rabbit Syntaxin17 antibodies and secondary antibodies conjugated to Alexa Fluor 488 and 647. 3D image stacks of syntaxin-17 and OxPhosV labels were obtained with the 60 \times (NA 1.4) Zeiss planapochromat objective of a III Yokogawa spinning disk confocal microscope. The percentage of syntaxin-17 label that overlapped a 3D mask of OxPhosV labeled mitochondria volumes was quantified using Slidebook image analysis software (III).

Ca^{2+} imaging

Cos7 cells were loaded with 5 μM Fura-2-AM or Rhod-2-AM in fresh medium containing 0.02% PAC for 45 or 30 min, respectively. Cells were perfused with normal buffer (125 mM NaCl, 20 mM HEPES pH 7.4, 5 mM KCl, 1.5 mM MgCl_2 and 10 mM glucose) containing 2.5 mM EGTA and images acquired with the 40 \times UAPO objective of an inverted Olympus IX71 microscope. Fura-2 was excited at 340 and 380 nm with a high-speed random access monochromator (Photon Technology International) and emission detected at 510 nm. Rhod-2 was excited at 545 nm and emission detected at 575 nm. Images were analyzed using InVivo Analyzer V3.0 software (Media Cybernetics). AMF decreases the $[\text{Ca}^{2+}]_{\text{cyt}}$ response (Fu et al., 2011) and only cells exhibiting equivalent $[\text{Ca}^{2+}]_{\text{cyt}}$ amplitudes were considered for calculation of coupling times.

Electron microscopy

Cells were grown as monolayers on Aclar film (Pelco), washed with PBS, fixed (2% glutaraldehyde in 0.1 M sodium cacodylate, pH 7.4 for 1 h), post-fixed (1% osmium tetroxide in cacodylate buffer for 1 h at 4°C), stained en bloc (0.1% uranyl acetate for 1 h) and progressively dehydrated through an ethanol series, followed by 100% acetone and embedding in Epon 812 (Fluka). Sections (50–60 nm thick; Leica Ultramicrotome) were stained with 2% uranyl acetate and 2% lead citrate, visualized on a FEI Tecnai G2 transmission electron microscope (acceleration voltage of 120 kV) and micrographs digitally recorded using an Eagle 4k CCD camera (FEI). Mitochondria perimeter and area measurements, and the length of SER and RER interfaces were measured to obtain the interface percentage using ImagePro 6.0 software. Widths of SER- and RER-mitochondria interfaces were determined by measuring the shortest distance between the ER membrane and the mitochondrial outer membrane at two sites for each contact.

Statistical analyses

Data are presented as mean \pm s.e.m. One-way ANOVA was used for group paired observations. Differences were considered statistically significant when $P < 0.05$.

Competing interests

The authors declare no competing or financial interests.

Author contributions

P.T.C.W. performed the fluorescence colocalization analysis and the quantitative analysis of the EM images. M.F. initiated colocalization and electron microscopy aspects of the project, the latter with N.P., and performed the Ca^{2+} measurements included in the paper. P.O.G. performed the EM analysis in the laboratory of N.P. M.M. helped with the EM quantification and P.S.-P. generated the tetracysteine Gp78 mutants used for the Ca^{2+} studies. I.R.N. directed the study and wrote the paper.

Funding

This study was supported by grants from the Canadian Institutes for Health Research (CIHR) [grant numbers COP-134057 and COP-137359 to I.R.N.]; the Canadian Breast Cancer Foundation to I.R.N.; and a grant from the National Science and Engineering Research Council (NSERC) to N.P. P.T.C.W. was the recipient of a UBC M.Sc. scholarship.

References

- Adams, S. R., Campbell, R. E., Gross, L. A., Martin, B. R., Walkup, G. K., Yao, Y., Llopis, J. and Tsien, R. Y. (2002). New biarsenical ligands and tetracysteine motifs for protein labeling in vitro and in vivo: synthesis and biological applications. *J. Am. Chem. Soc.* **124**, 6063–6076.
- Ballar, P., Zhong, Y., Nagahama, M., Tagaya, M., Shen, Y. and Fang, S. (2007). Identification of SVIP as an endogenous inhibitor of endoplasmic reticulum-associated degradation. *J. Biol. Chem.* **282**, 33908–33914.
- Benlimame, N., Simard, D. and Nabi, I. R. (1995). Autocrine motility factor receptor is a marker for a distinct membranous tubular organelle. *J. Cell Biol.* **129**, 459–471.
- Benlimame, N., Le, P. U. and Nabi, I. R. (1998). Localization of autocrine motility factor receptor to caveolae and clathrin-independent internalization of its ligand to smooth endoplasmic reticulum. *Mol. Biol. Cell* **9**, 1773–1786.
- Christianson, J. C., Olzmann, J. A., Shaler, T. A., Sowa, M. E., Bennett, E. J., Richter, C. M., Tyler, R. E., Greenblatt, E. J., Harper, J. W. and Kopito, R. R. (2011). Defining human ERAD networks through an integrative mapping strategy. *Nat. Cell Biol.* **14**, 93–105.

- Cosson, P., Marchetti, A., Ravazzola, M. and Orci, L. (2012). Mitofusin-2 independent juxtaposition of endoplasmic reticulum and mitochondria: an ultrastructural study. *PLoS ONE* **7**, e46293.
- Csordas, G., Renken, C., Varnai, P., Walter, L., Weaver, D., Buttle, K. F., Balla, T., Mannella, C. A. and Hajnoczky, G. (2006). Structural and functional features and significance of the physical linkage between ER and mitochondria. *J. Cell Biol.* **174**, 915-921.
- de Brito, O. M. and Scorrano, L. (2008). Mitofusin 2 tethers endoplasmic reticulum to mitochondria. *Nature* **456**, 605-610.
- Fang, S., Ferrone, M., Yang, C., Jensen, J. P., Tiwari, S. and Weissman, A. M. (2001). The tumor autocrine motility factor receptor, gp78, is a ubiquitin protein ligase implicated in degradation from the endoplasmic reticulum. *Proc. Natl. Acad. Sci. USA* **98**, 14422-14427.
- Filadi, R., Greotti, E., Turacchio, G., Luini, A., Pozzan, T. and Pizzo, P. (2015). Mitofusin 2 ablation increases endoplasmic reticulum-mitochondria coupling. *Proc. Natl. Acad. Sci. USA* **112**, E2174-E2181.
- Flourakis, M., Van Coppenolle, F., Lehen'kyi, V., Beck, B., Skryma, R. and Prevarskaya, N. (2006). Passive calcium leak via translocon is a first step for iPLA2-pathway regulated store operated channels activation. *FASEB J.* **20**, 1215-1217.
- Friedman, J. R., Lackner, L. L., West, M., DiBenedetto, J. R., Nunnari, J. and Voeltz, G. K. (2011). ER tubules mark sites of mitochondrial division. *Science* **334**, 358-362.
- Fu, M., Li, L., Albrecht, T., Johnson, J. D., Kojic, L. D. and Nabi, I. R. (2011). Autocrine motility factor/phosphoglucose isomerase regulates ER stress and cell death through control of ER calcium release. *Cell Death Differ.* **18**, 1057-1070.
- Fu, M., St-Pierre, P., Shankar, J., Wang, P. T. C., Joshi, B. and Nabi, I. R. (2013). Regulation of mitophagy by the Gp78 E3 ubiquitin ligase. *Mol. Biol. Cell* **24**, 1153-1162.
- Goetz, J. G., Genty, H., St-Pierre, P., Dang, T., Joshi, B., Sauvé, R., Vogl, W. and Nabi, I. R. (2007). Reversible interactions between smooth domains of the endoplasmic reticulum and mitochondria are regulated by physiological cytosolic Ca²⁺ levels. *J. Cell Sci.* **120**, 3553-3564.
- Hamasaki, M., Furuta, N., Matsuda, A., Nezu, A., Yamamoto, A., Fujita, N., Oomori, H., Noda, T., Haraguchi, T., Hiraoka, Y. et al. (2013). Autophagosomes form at ER-mitochondria contact sites. *Nature* **495**, 389-393.
- Ishihara, N., Eura, Y. and Mihara, K. (2004). Mitofusin 1 and 2 play distinct roles in mitochondrial fusion reactions via GTPase activity. *J. Cell Sci.* **117**, 6535-6546.
- Kojic, L. D., Joshi, B., Lajoie, P., Le, P. U., Cox, M. E., Turbin, D. A., Wiseman, S. A. and Nabi, I. R. (2007). Raft-dependent endocytosis of autocrine motility factor is phosphatidylinositol 3-kinase-dependent in breast carcinoma cells. *J. Biol. Chem.* **282**, 29305-29313.
- Korrmann, B., Currie, E., Collins, S. R., Schuldiner, M., Nunnari, J., Weissman, J. S. and Walter, P. (2009). An ER-mitochondria tethering complex revealed by a synthetic biology screen. *Science* **325**, 477-481.
- Le, P. U., Guay, G., Altschuler, Y. and Nabi, I. R. (2002). Caveolin-1 is a negative regulator of caveolae-mediated endocytosis to the endoplasmic reticulum. *J. Biol. Chem.* **277**, 3371-3379.
- Li, G., Zhao, G., Zhou, X., Schindelin, H. and Lennarz, W. J. (2006). The AAA ATPase p97 links peptide N-glycanase to the endoplasmic reticulum-associated E3 ligase autocrine motility factor receptor. *Proc. Natl. Acad. Sci. USA* **103**, 8348-8353.
- Lynes, E. M. and Simmen, T. (2011). Urban planning of the endoplasmic reticulum (ER): how diverse mechanisms segregate the many functions of the ER. *Biochim. Biophys. Acta* **1813**, 1893-1905.
- Mourier, A., Motori, E., Brandt, T., Lagouge, M., Atanassov, I., Galinier, A., Rapp, G., Brodesser, S., Hultenby, K., Dieterich, C. et al. (2015). Mitofusin 2 is required to maintain mitochondrial coenzyme Q levels. *J. Cell Biol.* **208**, 429-442.
- Nabi, I. R., Watanabe, H. and Raz, A. (1990). Identification of B16-F1 melanoma autocrine motility-like factor receptor. *Cancer Res.* **50**, 409-414.
- Pacher, P., Sharma, K., Csordas, G., Zhu, Y. and Hajnoczky, G. (2008). Uncoupling of ER-mitochondrial calcium communication by transforming growth factor-beta. *Am. J. Physiol. Renal Physiol.* **295**, F1303-F1312.
- Rambold, A. S., Kostecky, B., Elia, N. and Lippincott-Schwartz, J. (2011). Tubular network formation protects mitochondria from autophagosomal degradation during nutrient starvation. *Proc. Natl. Acad. Sci. USA* **108**, 10190-10195.
- Rapizzi, E., Pinton, P., Szabadkai, G., Wieckowski, M. R., Vandecasteele, G., Baird, G., Tuft, R. A., Fogarty, K. E. and Rizzuto, R. (2002). Recombinant expression of the voltage-dependent anion channel enhances the transfer of Ca²⁺ microdomains to mitochondria. *J. Cell Biol.* **159**, 613-624.
- Rowland, A. A. and Voeltz, G. K. (2012). Endoplasmic reticulum-mitochondria contacts: function of the junction. *Nat. Rev. Mol. Cell Biol.* **13**, 607-625.
- Schumacher, M. M., Choi, J.-Y. and Voelker, D. R. (2002). Phosphatidylserine transport to the mitochondria is regulated by ubiquitination. *J. Biol. Chem.* **277**, 51033-51042.
- Shankar, J., Kojic, L. D., St-Pierre, P., Wang, P. T. C., Fu, M., Joshi, B. and Nabi, I. R. (2013). Raft endocytosis of AMF regulates mitochondrial dynamics through Rac1 signaling and the Gp78 ubiquitin ligase. *J. Cell Sci.* **126**, 3295-3304.
- Silletti, S., Watanabe, H., Hogan, V., Nabi, I. R. and Raz, A. (1991). Purification of B16-F1 melanoma autocrine motility factor and its receptor. *Cancer Res.* **51**, 3301-3311.
- Simmen, T., Aslan, J. E., Blagoveshchenskaya, A. D., Thomas, L., Wan, L., Xiang, Y., Feliciangeli, S. F., Hung, C.-H., Crump, C. M. and Thomas, G. (2005). PACS-2 controls endoplasmic reticulum-mitochondria communication and Bid-mediated apoptosis. *EMBO J.* **24**, 717-729.
- Song, B.-L., Sever, N. and DeBose-Boyd, R. A. (2005). Gp78, a membrane-anchored ubiquitin ligase, associates with Insig-1 and couples sterol-regulated ubiquitination to degradation of HMG CoA reductase. *Mol. Cell* **19**, 829-840.
- St-Pierre, P., Dang, T., Joshi, B. and Nabi, I. R. (2012). Peripheral endoplasmic reticulum localization of the gp78 ubiquitin ligase activity. *J. Cell Sci.* **125**, 1727-1737.
- Szabadkai, G., Bianchi, K., Varnai, P., De Stefani, D., Wieckowski, M. R., Cavagna, D., Nagy, A. I., Balla, T. and Rizzuto, R. (2006). Chaperone-mediated coupling of endoplasmic reticulum and mitochondrial Ca²⁺ channels. *J. Cell Biol.* **175**, 901-911.
- Tsai, Y. C., Mendoza, A., Mariano, J. M., Zhou, M., Kostova, Z., Chen, B., Veenstra, T., Hewitt, S. M., Helman, L. J., Khanna, C. et al. (2007). The ubiquitin ligase gp78 promotes sarcoma metastasis by targeting KAI1 for degradation. *Nat. Med.* **13**, 1504-1509.
- Tsutsumi, S., Hogan, V., Nabi, I. R. and Raz, A. (2003). Overexpression of the autocrine motility factor/phosphoglucose isomerase induces transformation and survival of NIH-3T3 fibroblasts. *Cancer Res.* **63**, 242-249.
- Wang, H.-J., Guay, G., Pogan, L., Sauve, R. and Nabi, I. R. (2000). Calcium regulates the association between mitochondria and a smooth subdomain of the endoplasmic reticulum. *J. Cell Biol.* **150**, 1489-1498.
- Ye, Y., Shibata, Y., Kikkert, M., van Voorden, S., Wiertz, E. and Rapoport, T. A. (2005). Recruitment of the p97 ATPase and ubiquitin ligases to the site of retrotranslocation at the endoplasmic reticulum membrane. *Proc. Natl. Acad. Sci. USA* **102**, 14132-14138.
- Zhong, X., Shen, Y., Ballar, P., Apostolou, A., Agami, R. and Fang, S. (2004). AAA ATPase p97/valosin-containing protein interacts with gp78, a ubiquitin ligase for endoplasmic reticulum-associated degradation. *J. Biol. Chem.* **279**, 45676-45684.